

Higgs pair production in the ElectroWeak Chiral Lagrangian framework

Matteo Capozzi

G. Buchalla, A. Celis, G. Heinrich, L. Scyboz [[arXiv:1806.05162](https://arxiv.org/abs/1806.05162)]

Max-Planck-Institut
für Physik



12/07/2018
Munich

Outline

- Motivation
- ElectroWeak Chiral Lagrangian framework
- Results
- Conclusions

Motivation

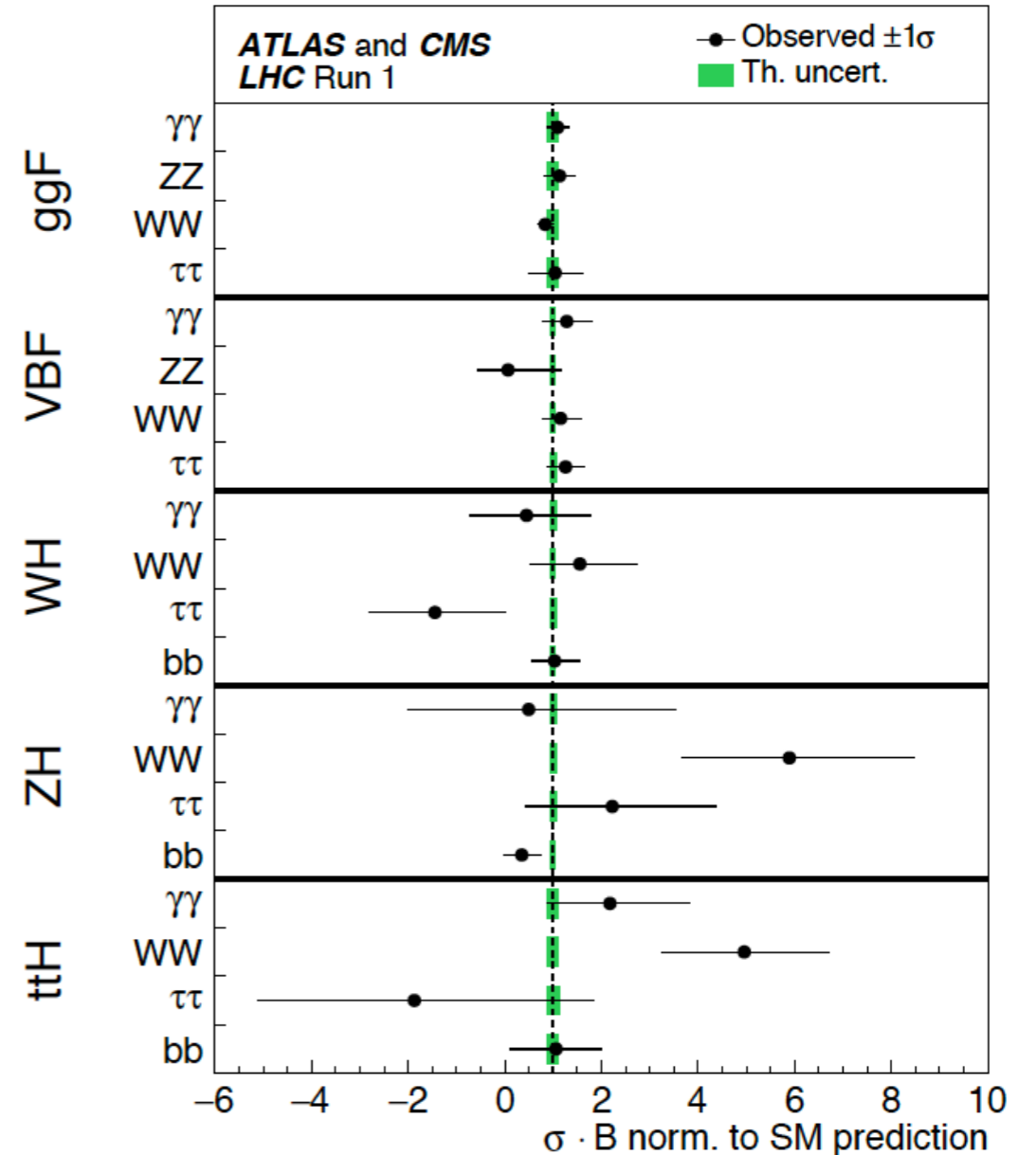
- Discovery of the Higgs boson: most important element in our understanding of electroweak symmetry breaking.
- The hierarchy problem and other open questions in the SM motivate us to explore extensions to the Higgs sector.
- SM is very well tested. If there are new physics effects they are likely to show up in the Higgs sector, but no evidence of new physics has been found up to date.
- New physics may hide at higher scales, therefore a low energy approximation of new physics can allow us to parametrize new physics contributions.
- So we work in an Effective Field Theory (EFT) framework, in particular the one provided by the ElectroWeak Chiral Lagrangian (EWChL) [Buchalla et al. [arXiv:1307.5017](https://arxiv.org/abs/1307.5017)].

Motivation

- EWChL provides a non linear realization of the electroweak symmetry breaking sector.
- Many of the Higgs couplings are well constrained already or can be obtained from other processes, but this is not true for the Higgs boson self coupling.
- Non standard couplings in the Higgs sector in principle can be large in this framework. Therefore we only consider the Higgs sector within the EWChL framework, in particular Higgs boson pair production.
- We focus on the gluon fusion channel , the channel with the biggest cross section.

$$L_{gg \rightarrow hh} \supset -m_t \bar{t}t \left(c_{tth} \frac{h}{v} + c_{ttth} \frac{h^2}{2v^2} \right) - c_{hhh} \frac{1}{6} \left(\frac{3m_h^2}{v} \right) h^3$$

$$+ \frac{g_s^2}{16\pi^2} \langle G_{\mu\nu} G^{\mu\nu} \rangle \left(c_{ghh} \frac{h}{v} + c_{gghh} \frac{h^2}{2v^2} \right)$$



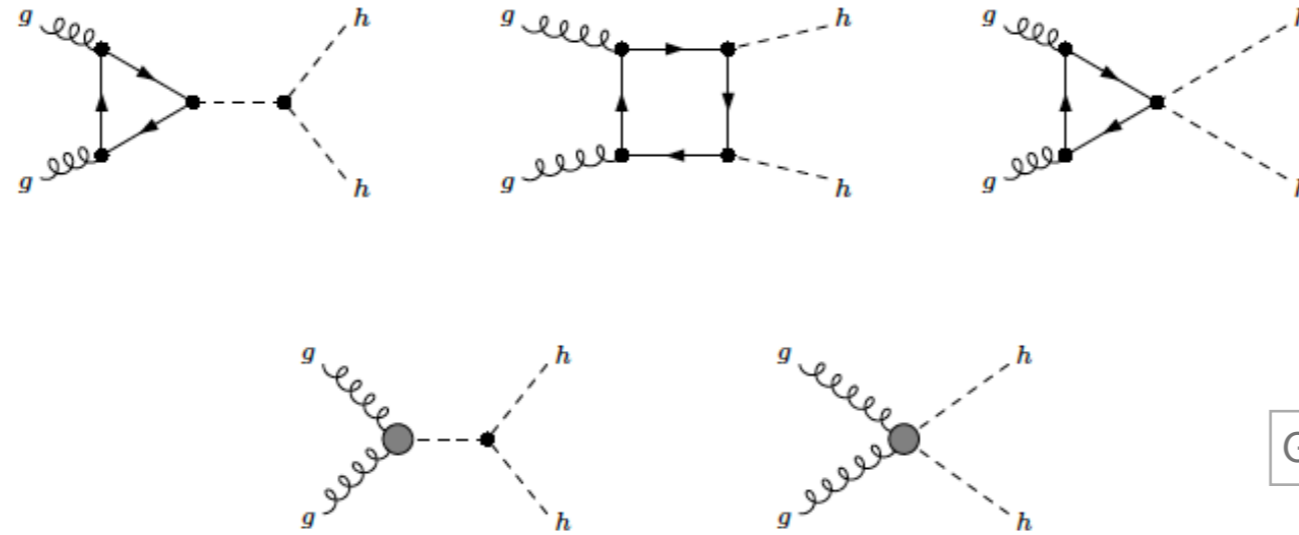
ATLAS, CMS collaboration
[arXiv:1606.02266](https://arxiv.org/abs/1606.02266)

EFT + higher order QCD $gg \rightarrow HH$ brief state of art

- Cross section parametrization within EFT framework see e.g. [Azatov et al. [arXiv:1502.00539](#)].
- NLO HEFT calculation based on dimension 6 operators [Gröber et al. [arXiv:1504.06577](#)], including CP violating terms [Gröber et al. [arXiv:1705.05314](#)].
- NNLO HEFT results including dimension 6 operators [de Florian et al. [arXiv:1704.05700](#)].
- Presentation of Benchmark points in order to explore the BSM parameters space see e.g. [Carvalho et al. [arXiv:1507.02245](#)].
- NLO SM full top mass dependent calculation including variation of the Higgs self coupling [Borowka et al. [arXiv:1608.04798](#)].

EWChL for $gg \rightarrow HH$

- At leading order there are 5 different diagrams: 2 SM-like diagrams and 3 totally new diagrams.



Gröber et al. [arXiv:1504.06577](https://arxiv.org/abs/1504.06577)

- The Feynman amplitude of this process can be written as:

$$M^{\mu\nu} = F_1 T_1^{\mu\nu} + F_2 T_2^{\mu\nu}$$

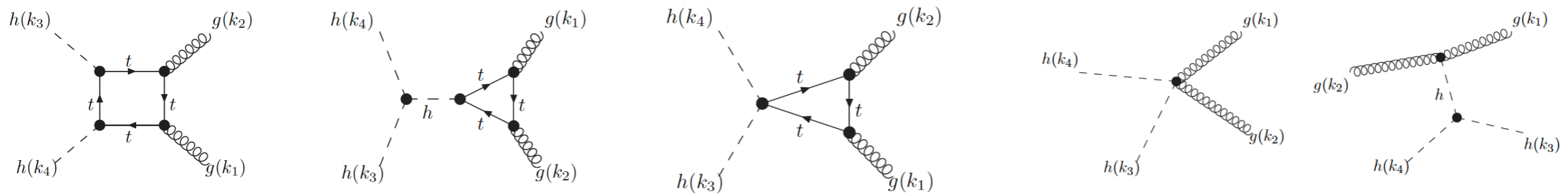
$$T_1^{\mu\nu} = -g^{\mu\nu} + \frac{k_1^\nu k_2^\mu}{(k_1 \cdot k_2)} \quad T_2^{\mu\nu} = g^{\mu\nu} + \frac{1}{k_T^2 (k_1 \cdot k_2)} (m_h^2 k_1^\nu k_2^\mu - 2(k_1 \cdot k_3) k_3^\nu k_2^\mu - 2(k_2 \cdot k_3) k_3^\mu k_1^\nu) + 2(k_1 \cdot k_2) k_3^\mu k_3^\nu$$

- In order to compute the deviations of the model, we need to know the contributions of these new diagrams to the form factors F_1 and F_2 .

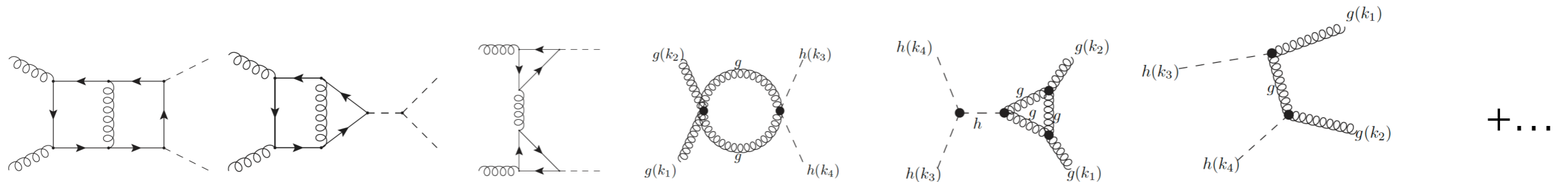
$$\hat{\sigma}^{LO} = \frac{\alpha_s^2}{2^{12} v^4 (2\pi)^3 \hat{s}^2} \int_{\hat{t}_-}^{\hat{t}_+} d\hat{t} \{ |F_1|^2 + |F_2|^2 \}$$

gg→HH contributions in the EWChL framework

Leading order

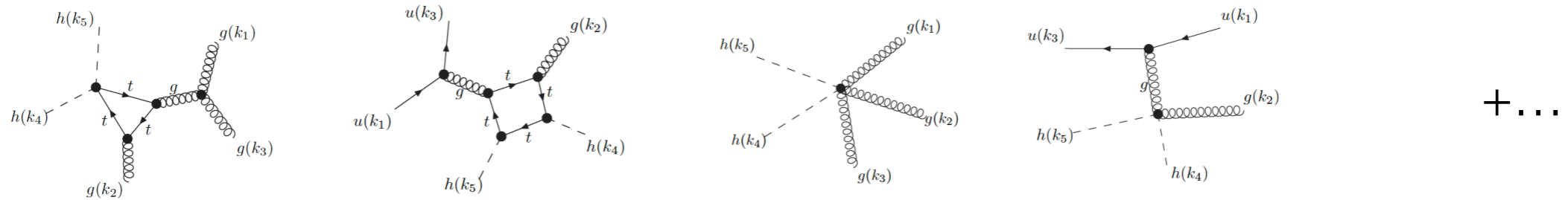


NLO QCD virtual



NLO QCD real

Borowka et al. arXiv:1608.04798



Method of the calculation

- In order to obtain the LO QCD cross section and the NLO QCD real corrections we used a C++ code linked to the automated one loop generator GoSam [Cullen et al. [arXiv:1404.7096](#)].
- For the NLO QCD virtual correction we used the two-loop integrals computed numerically (using the program SecDec) for the SM case [Borowka et al. [arXiv:1608.04798](#)].
- Within our setup we can produce the full top mass dependent NLO QCD cross section and differential distributions.
- In the following we will show distributions for some of the benchmark points and compare them with SM results.

Benchmark points

- Benchmark points introduced in Carvalho et al. [[arXiv:1507.02245](#), [arXiv:1608.06578](#) and [arXiv:1710.08261](#)], calculating LO distributions.
- The aim of the benchmark points is to probe the BSM couplings space.
- According to the values of the five anomalous couplings the shape of the differential distribution can change.
- The idea of the benchmark points is to define 12 clusters with different shapes, which characterize distributions attributed to a given choice of couplings.
- We produced the inclusive and differential cross sections at NLO with full top mass dependence.

Benchmark	C_{hhh}	C_t	C_{tt}	C_{ggh}	C_{gggh}
1	7.5	1.0	-1.0	0.0	0.0
2	1.0	1.0	0.5	$-\frac{1.6}{3}$	-0.2
3	1.0	1.0	-1.5	0.0	$\frac{0.8}{3}$
4	-3.5	1.5	-3.0	0.0	0.0
5	1.0	1.0	0.0	$\frac{1.6}{3}$	$\frac{1.0}{3}$
6	2.4	1.0	0.0	$\frac{0.4}{3}$	$\frac{0.2}{3}$
7	5.0	1.0	0.0	$\frac{0.4}{3}$	$\frac{0.2}{3}$
8a	1.0	1.0	0.5	$\frac{0.8}{3}$	0.0
9	1.0	1.0	1.0	-0.4	-0.2
10	10.0	1.5	-1.0	0.0	0.0
11	2.4	1.0	0.0	$\frac{2.0}{3}$	$\frac{1.0}{3}$
12	15.0	1.0	1.0	0.0	0.0
SM	1.0	1.0	0.0	0.0	0.0

Benchmark points

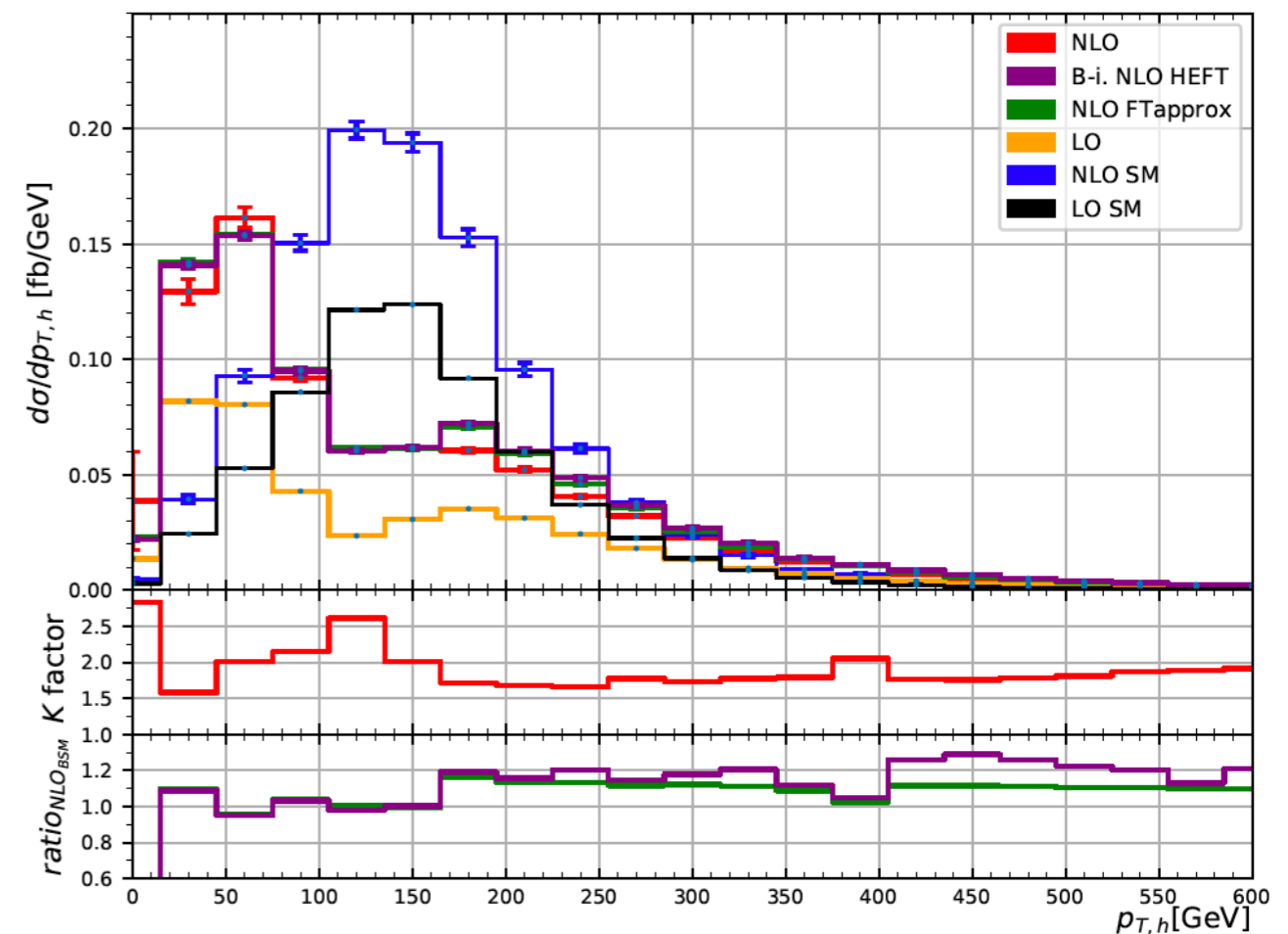
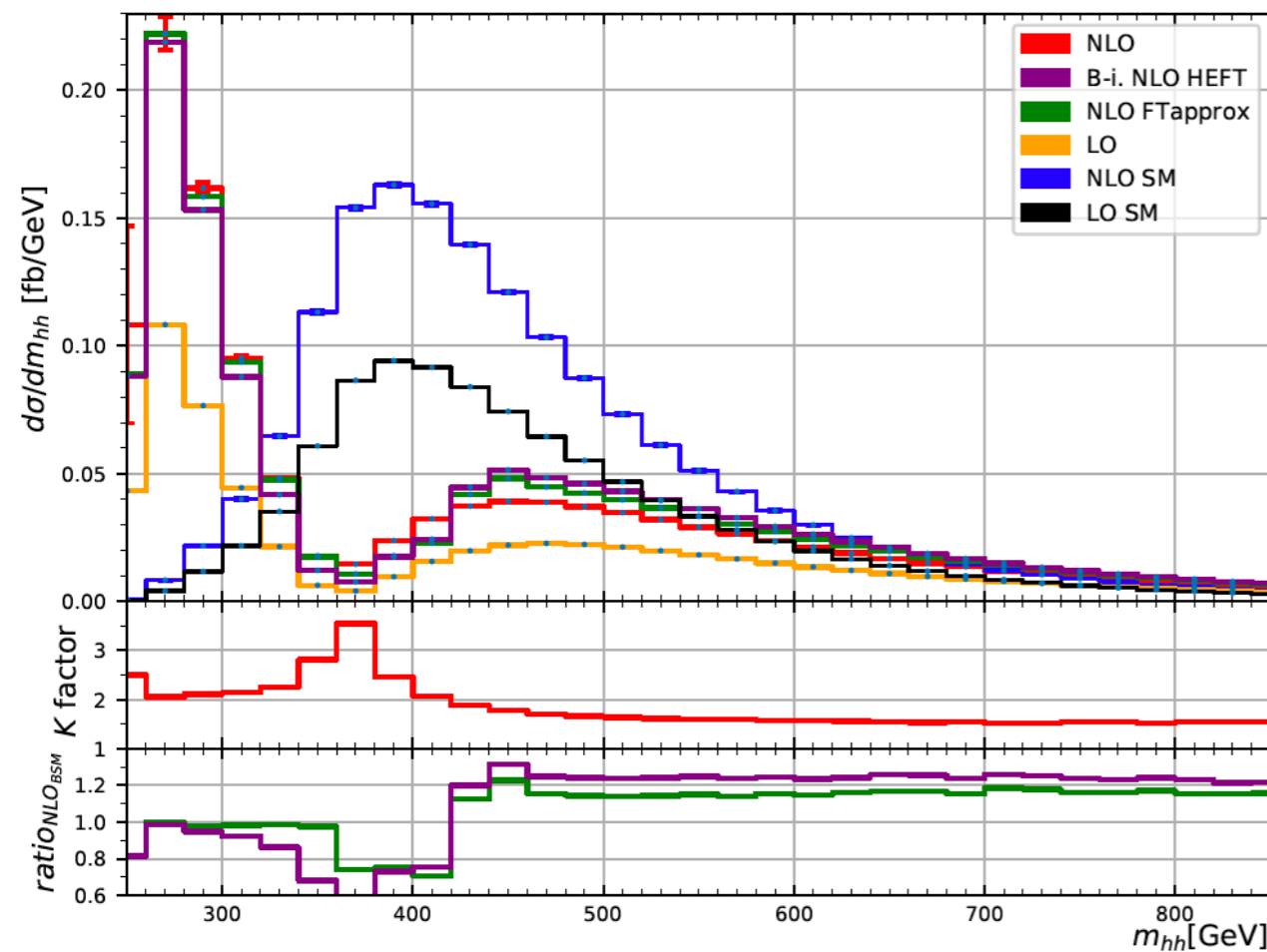
Benchmark	σ_{NLO} [fb]	K-factor	scale uncert. [%]	stat. uncert. [%]	$\frac{\sigma_{NLO}}{\sigma_{NLO,SM}}$
B_1	194.89	1.88	+19 -15	1.6	5.915
B_2	14.55	1.88	+5 -13	0.56	0.4416
B_3	1047.37	1.98	+21 -16	0.15	31.79
B_4	8922.75	1.98	+19 -16	0.39	270.8
B_5	59.325	1.83	+4 -15	0.36	1.801
B_6	24.69	1.89	+2 -11	2.1	0.7495
B_7	169.41	2.07	+9 -12	2.2	5.142
B_{8a}	41.70	2.34	+6 -9	0.63	1.266
B_9	146.00	2.30	+22 -16	0.31	4.431
B_{10}	575.86	2.00	+17 -14	3.2	17.48
B_{11}	174.70	1.92	+24 -8	1.2	5.303
B_{12}	3618.53	2.07	+16 -15	1.2	109.83
SM	32.95	1.66	+14 -13	0.1	1

- Some of them already ruled out [[arXiv:1806.00408](https://arxiv.org/abs/1806.00408)].

Benchmark points: m_{hh} and $p_{T,h}$ distributions

Benchmark 6

$$\frac{\sigma_{NLO}}{\sigma_{NLO,SM}} = 0.7495$$

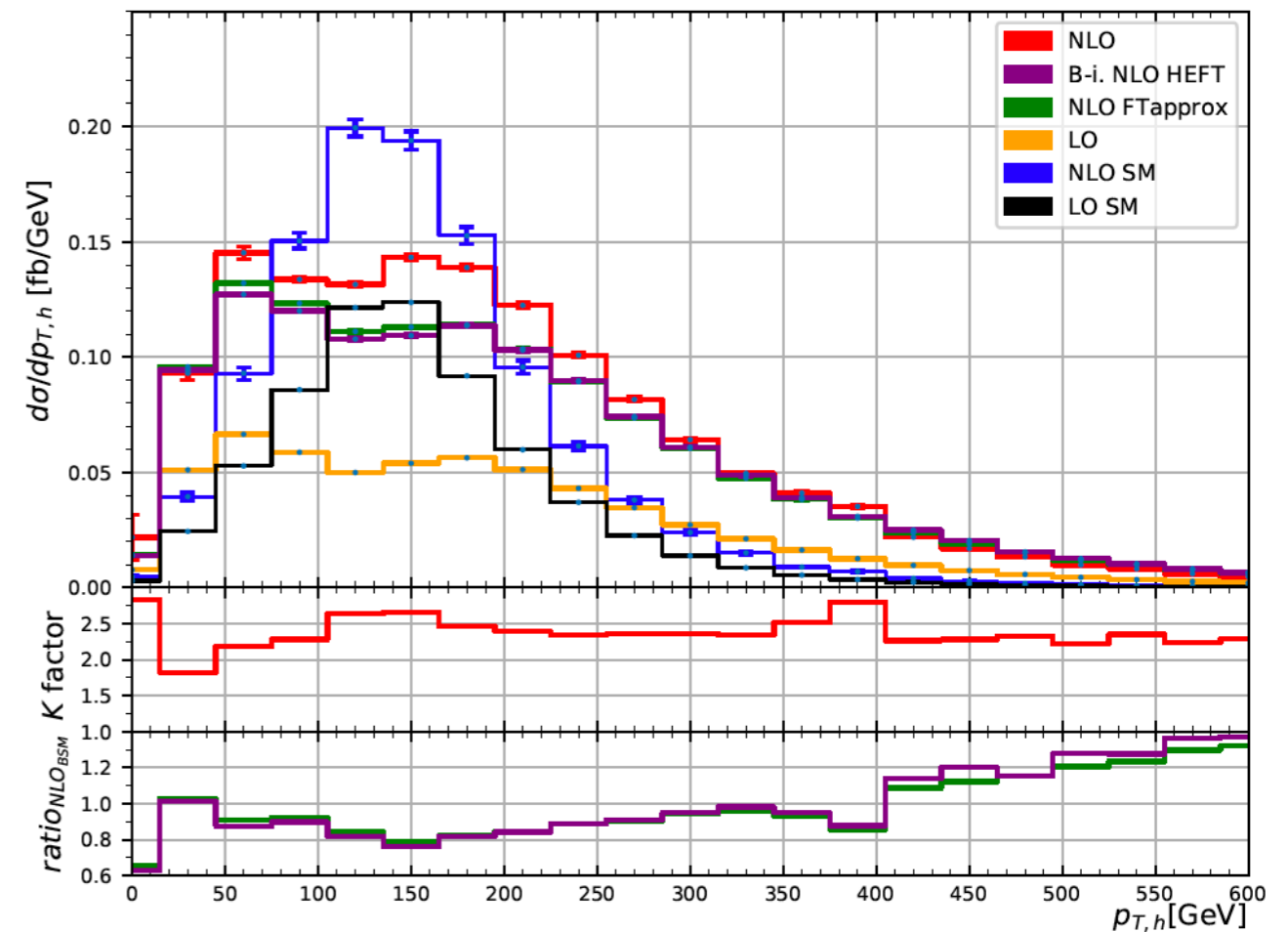
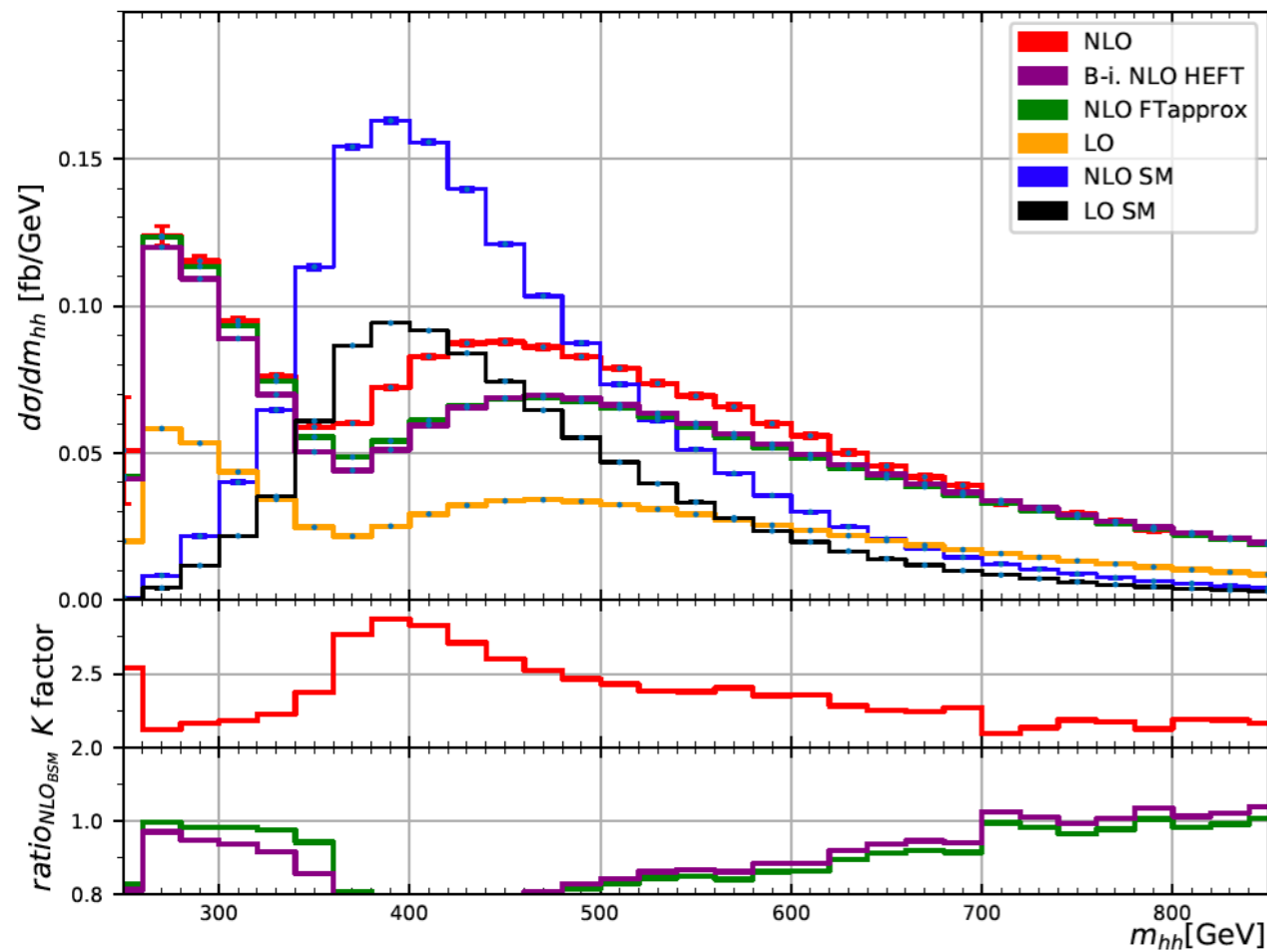


$$c_{hhh} = 2.4, c_t = 1.0, c_{tt} = 0, c_{ggh} = \frac{0.4}{3}, c_{gghh} = \frac{0.2}{3}$$

Benchmark points: m_{hh} and $p_{T,h}$ distributions

Benchmark 8-a

$$\frac{\sigma_{NLO}}{\sigma_{NLO,SM}} = 1.266$$

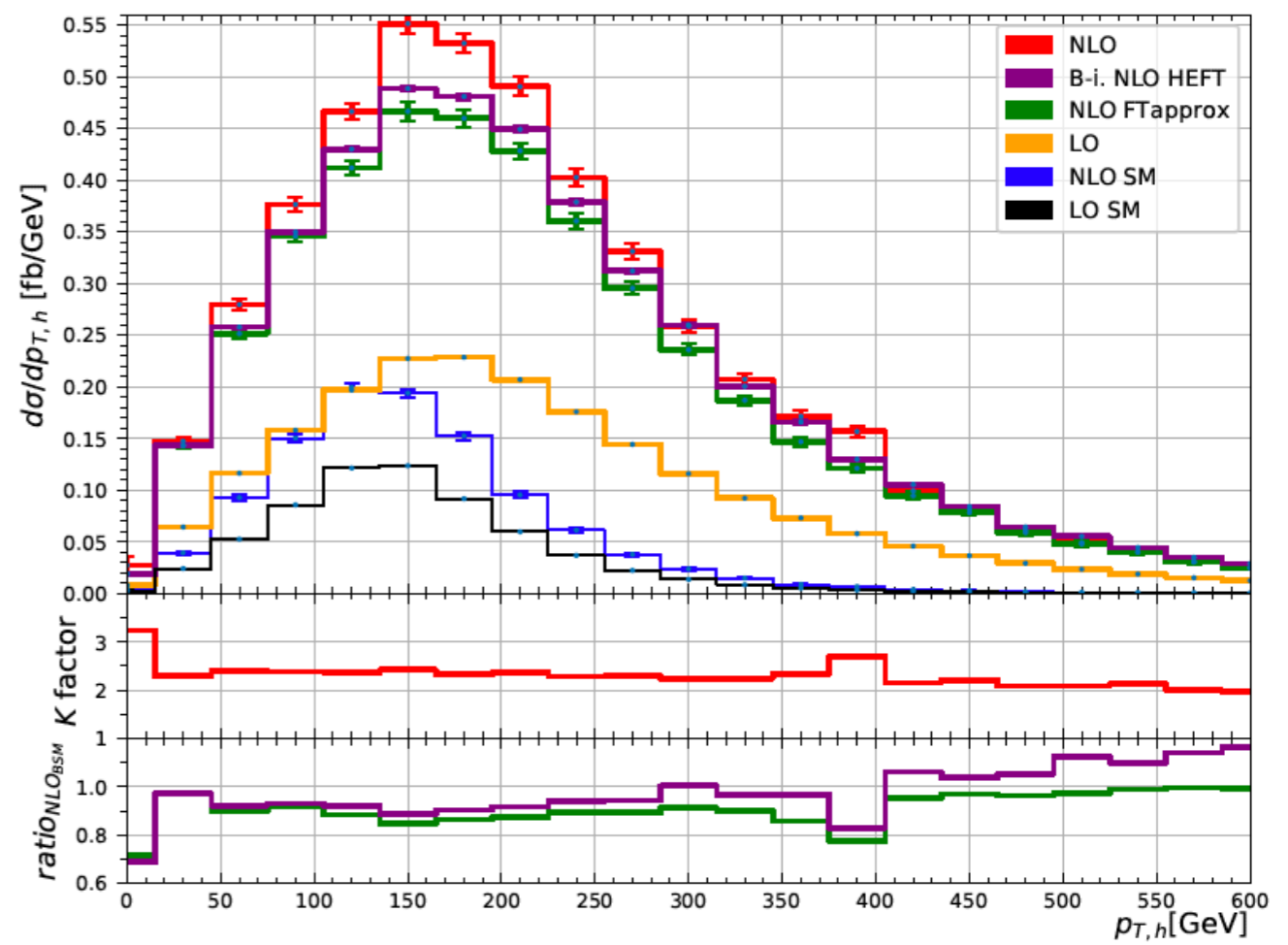
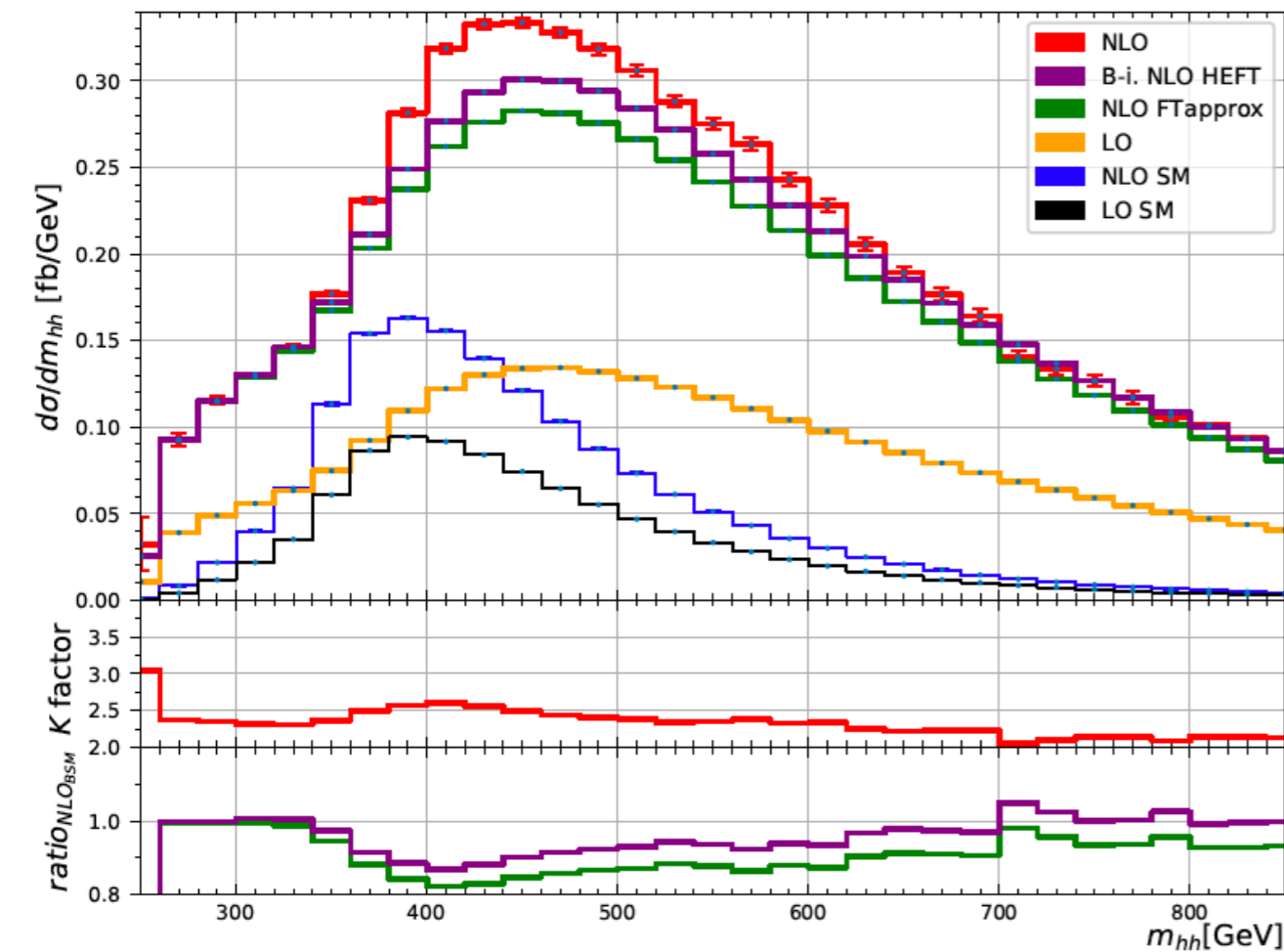


$$c_{hhh} = 1.0, c_t = 1.0, c_{tt} = 0.5, c_{ggh} = \frac{0.8}{3}, c_{gghh} = 0$$

Benchmark points: m_{hh} and $p_{T,h}$ distributions

Benchmark 9

$$\frac{\sigma_{NLO}}{\sigma_{NLO,SM}} = 4.431$$



$$c_{hhh} = 1.0, c_t = 1.0, c_{tt} = 1.0, c_{ggh} = -0.4, c_{gggh} = -0.2$$

Cross section fit

- In general the LO cross section for the process can be parametrized as function of the 5 BSM couplings in terms of 15 parameters.

$$\begin{aligned} \frac{\sigma_{LO}}{\sigma_{LO,SM}} = & [A_1 c_t^4 + A_2 c_{tt}^2 + A_3 c_{thh}^2 c_{hhh}^2 + A_4 c_{ghh}^2 c_{hhh}^2 + A_5 c_{gghh}^2 + A_6 c_{tt} c_t^2 + A_7 c_t^3 c_{hhh} \\ & + A_8 c_{tt} c_t c_{hhh} + A_9 c_{tt} c_{ggh} c_{hhh} + A_{10} c_{tt} c_{cgghh} + A_{11} c_t^2 c_{ggh} c_{hhh} + A_{12} c_t^2 c_{gghh} \\ & + A_{13} c_t c_{hhh}^2 c_{gghh} + A_{14} c_t c_{hhh} c_{gghh} + A_{15} c_{ggh} c_{hhh} c_{gghh}] \end{aligned}$$

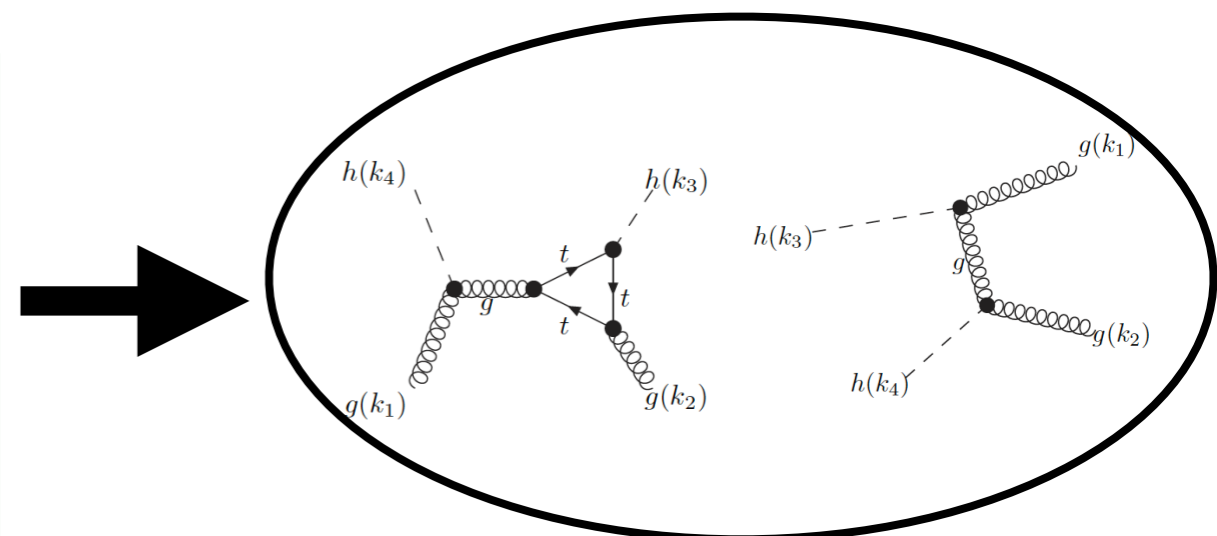
- We determined the value of the 15 parameters via projections. We evaluated the cross section for 15 different combinations of the couplings in order to obtain a system of 15 equations. The values of the parameters are the solutions of the system.
- We checked our results with the ones of Azatov et al. [[arXiv:1502.00539](https://arxiv.org/abs/1502.00539)] and found agreement.
- At NLO QCD the 15 coefficients change plus there are 8 new ones.

$$\begin{aligned} \frac{\sigma_{NLO}}{\sigma_{NLO,SM}} = & [A'_1 c_t^4 + A'_2 c_{tt}^2 + A'_3 c_{thh}^2 c_{hhh}^2 + A'_4 c_{ghh}^2 c_{hhh}^2 + A'_5 c_{gghh}^2 + A'_6 c_{tt} c_t^2 + A'_7 c_t^3 c_{hhh} \\ & + A'_8 c_{tt} c_t c_{hhh} + A'_9 c_{tt} c_{ggh} c_{hhh} + A'_{10} c_{tt} c_{cgghh} + A'_{11} c_t^2 c_{ggh} c_{hhh} + A'_{12} c_t^2 c_{gghh} \\ & + A'_{13} c_t c_{hhh}^2 c_{gghh} + A'_{14} c_t c_{hhh} c_{gghh} + A'_{15} c_{ggh} c_{hhh} c_{gghh} + \underline{A'_{16} c_t^3 c_{ggh} + A'_{17} c_t c_{tt} c_{ggh}} \\ & + \underline{A'_{18} c_t c_{ggh}^2 c_{hhh} + A'_{19} c_t c_{ggh} c_{gghh} + A'_{20} c_t^2 c_{ggh}^2 + A'_{21} c_{tt} c_{ggh}^2 + A_{22} c_{ggh}^3 c_{hhh} + A'_{23} c_{ggh}^2 c_{gghh}}] \end{aligned}$$

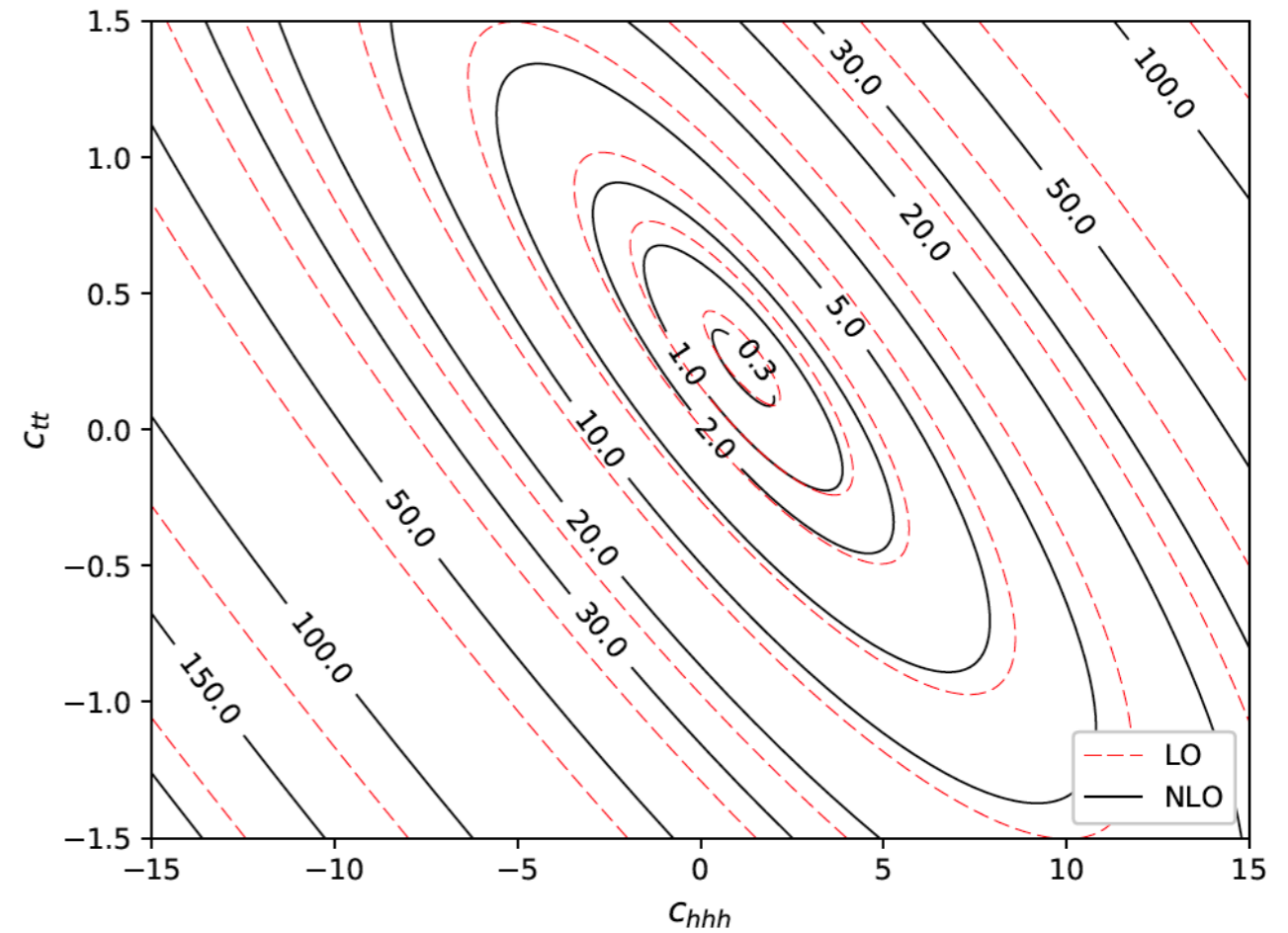
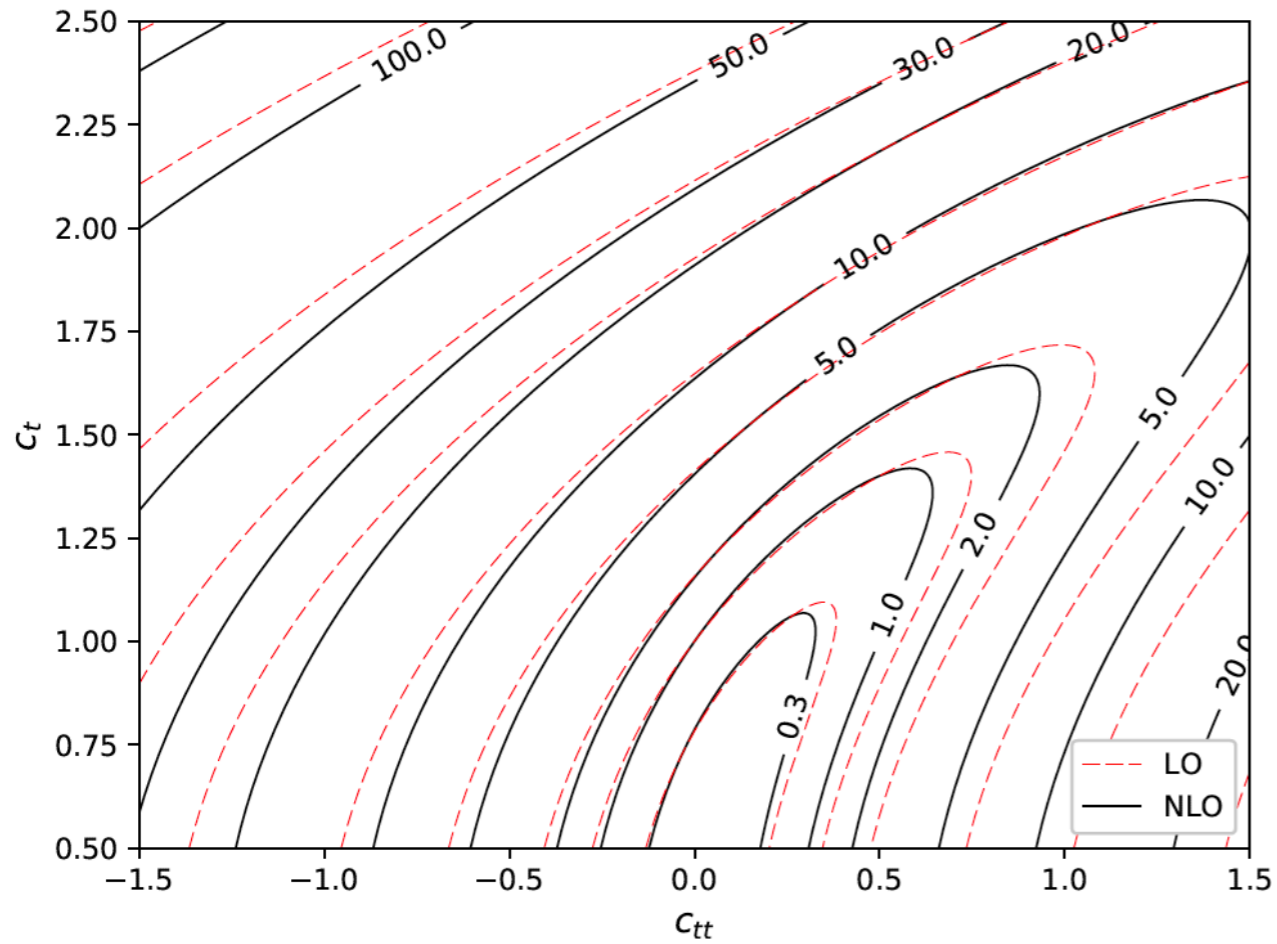
Cross section fit

A coeff	LO value	LO uncertainty	NLO value	NLO uncertainty
A_1	2.08059	0.00163127	2.23389	0.0100989
A_2	10.2011	0.00809032	12.4598	0.0424131
A_3	0.27814	0.00187658	0.342248	0.0153637
A_4	0.314043	0.000312416	0.346822	0.00327358
A_5	12.2731	0.0101351	13.0087	0.0962361
A_6	-8.49307	0.00885261	-9.6455	0.0503776
A_7	-1.35873	0.00148022	-1.57553	0.0136033
A_8	2.80251	0.0130855	3.43849	0.0771694
A_9	2.48018	0.0127927	2.86694	0.0772341
A_{10}	14.6908	0.0311171	16.6912	0.178501
A_{11}	-1.15916	0.00307598	-1.25293	0.0291153
A_{12}	-5.51183	0.0131254	-5.81216	0.134029
A_{13}	0.560503	0.00339209	0.649714	0.0287388
A_{14}	2.47982	0.0190299	2.85933	0.193023
A_{15}	2.89431	0.0157818	3.14475	0.148658
A_{16}			-0.00816241	0.000224985
A_{17}			0.0208652	0.000398929
A_{18}			0.0168157	0.00078306
A_{19}			0.0298576	0.000829474
A_{20}			-0.0270253	0.000701919
A_{21}			0.0726921	0.0012875
A_{22}			0.0145232	0.000703893
A_{23}			0.123291	0.00650551

- We present the results for the coefficients at LO and NLO.
- Using the fitted cross section we study the behavior of the cross section as a function of the BSM parameters.
- We show some of the iso-contours produced using the fit.

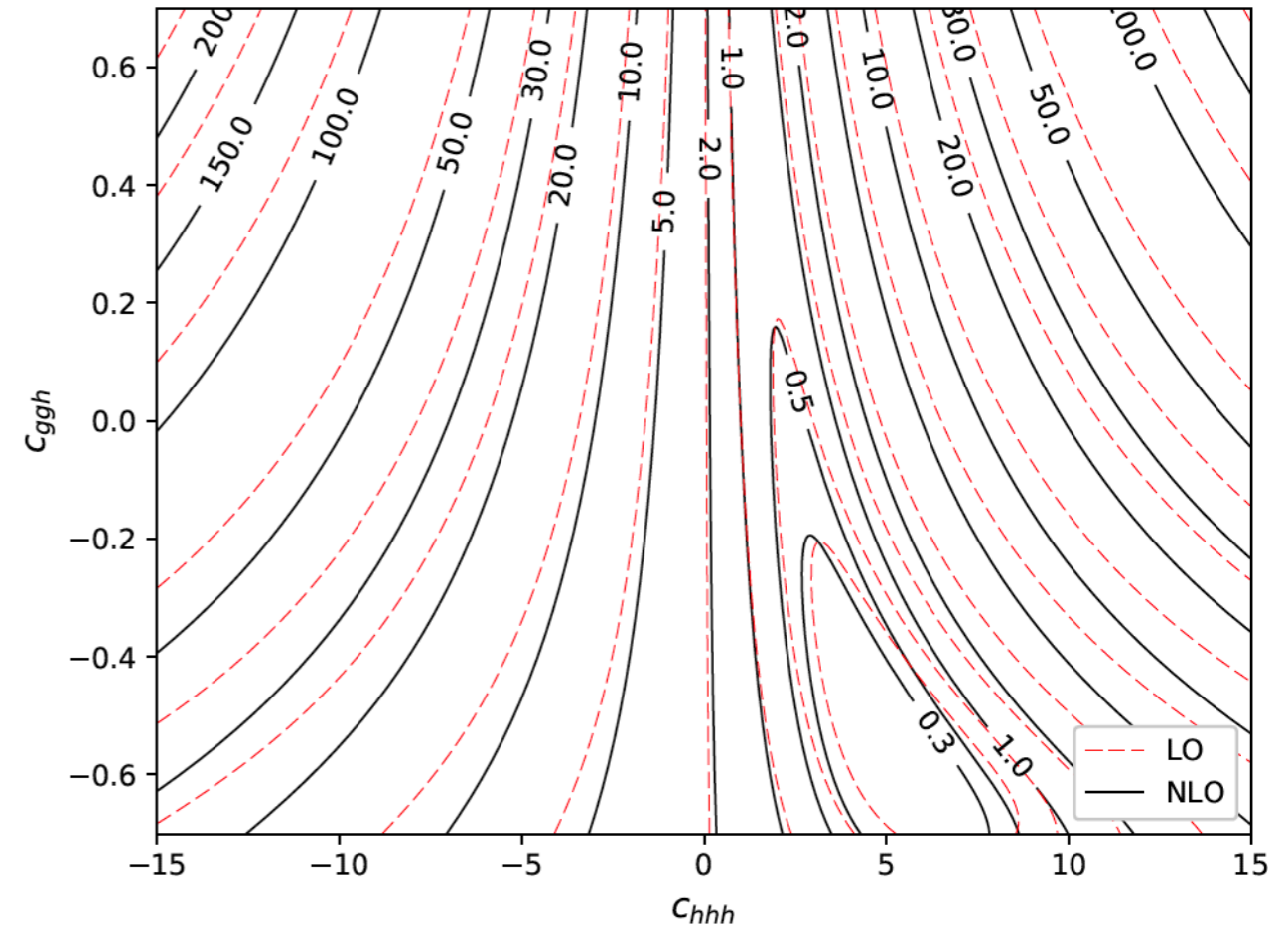
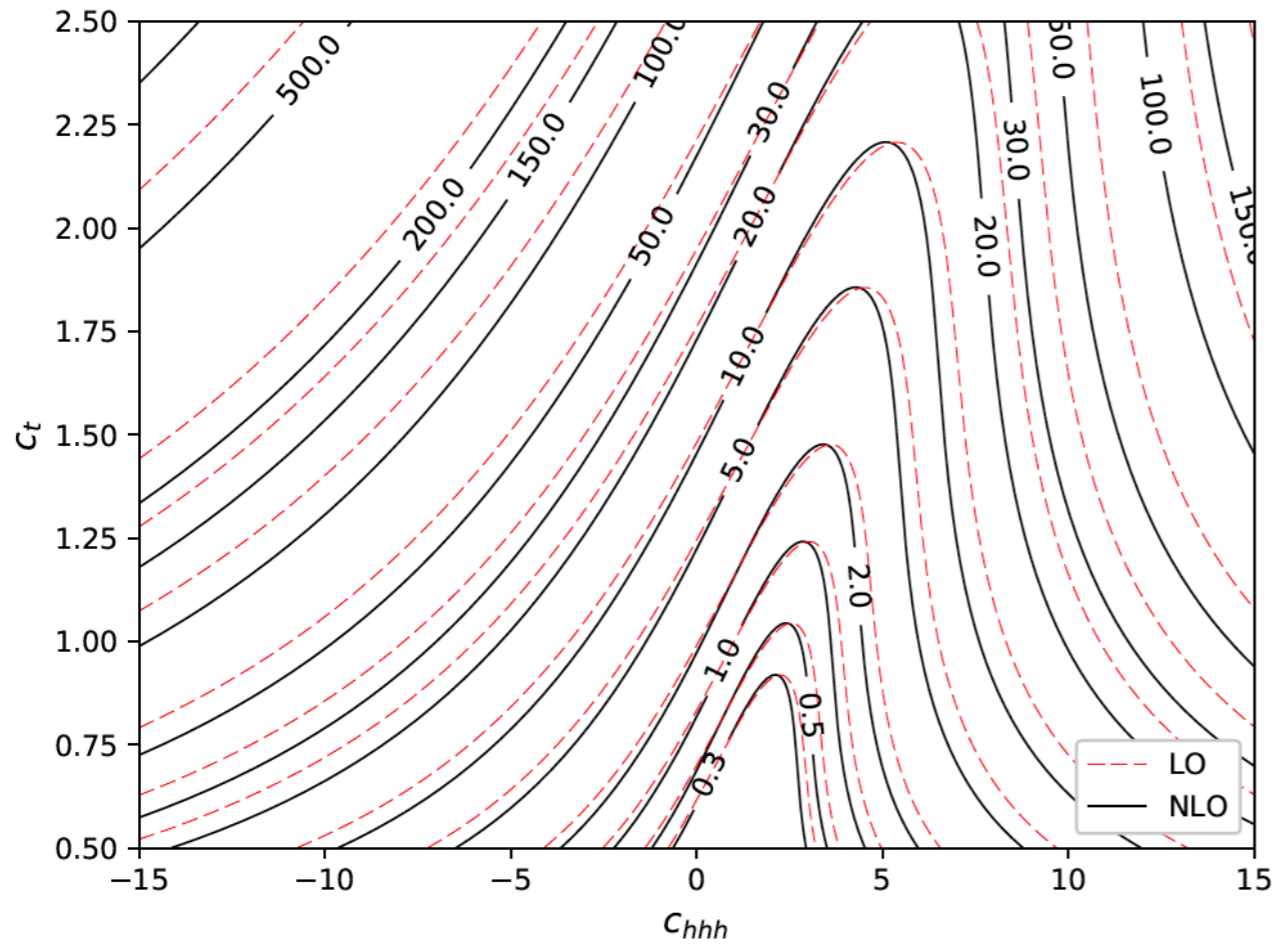


NLO Iso-contours



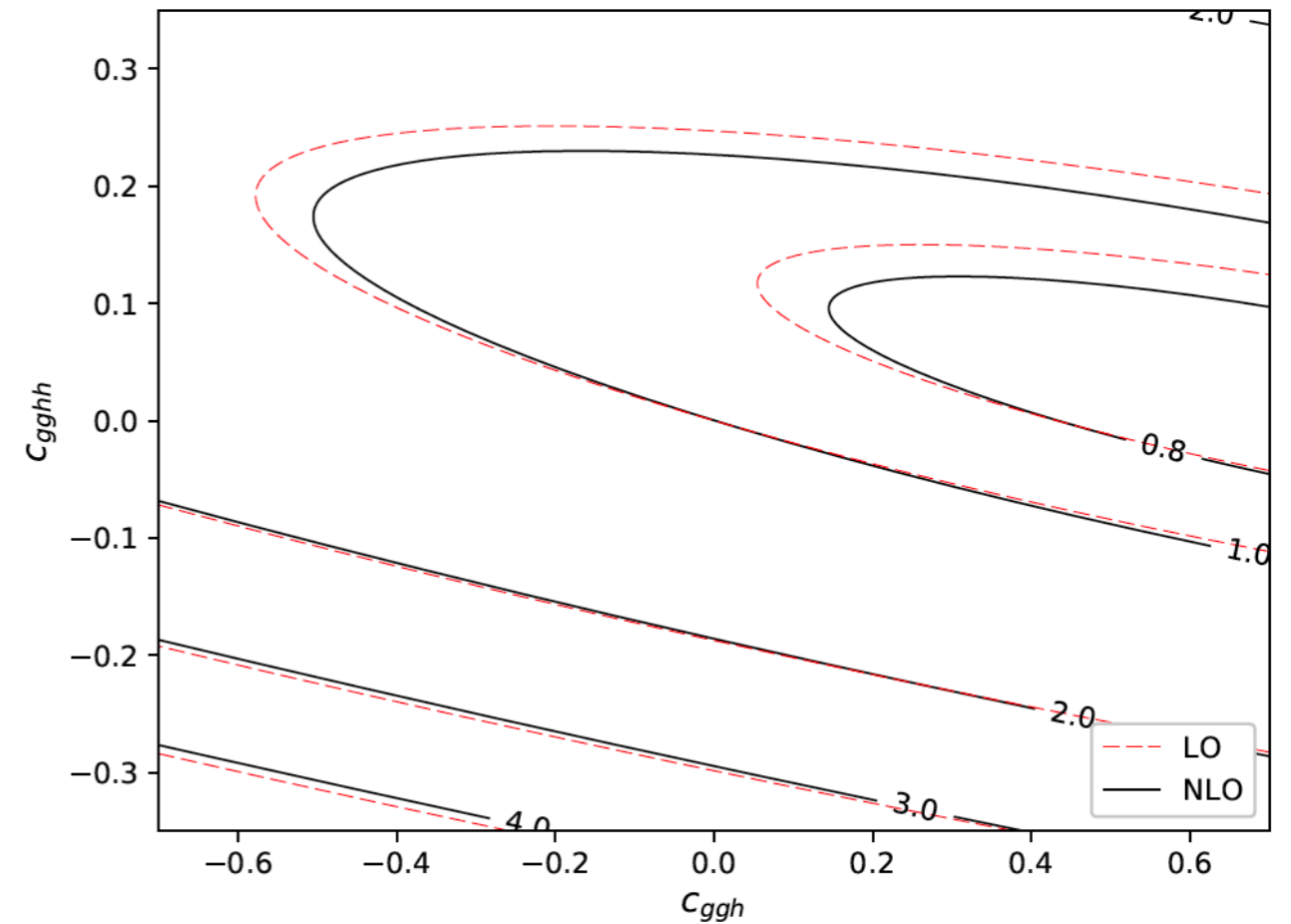
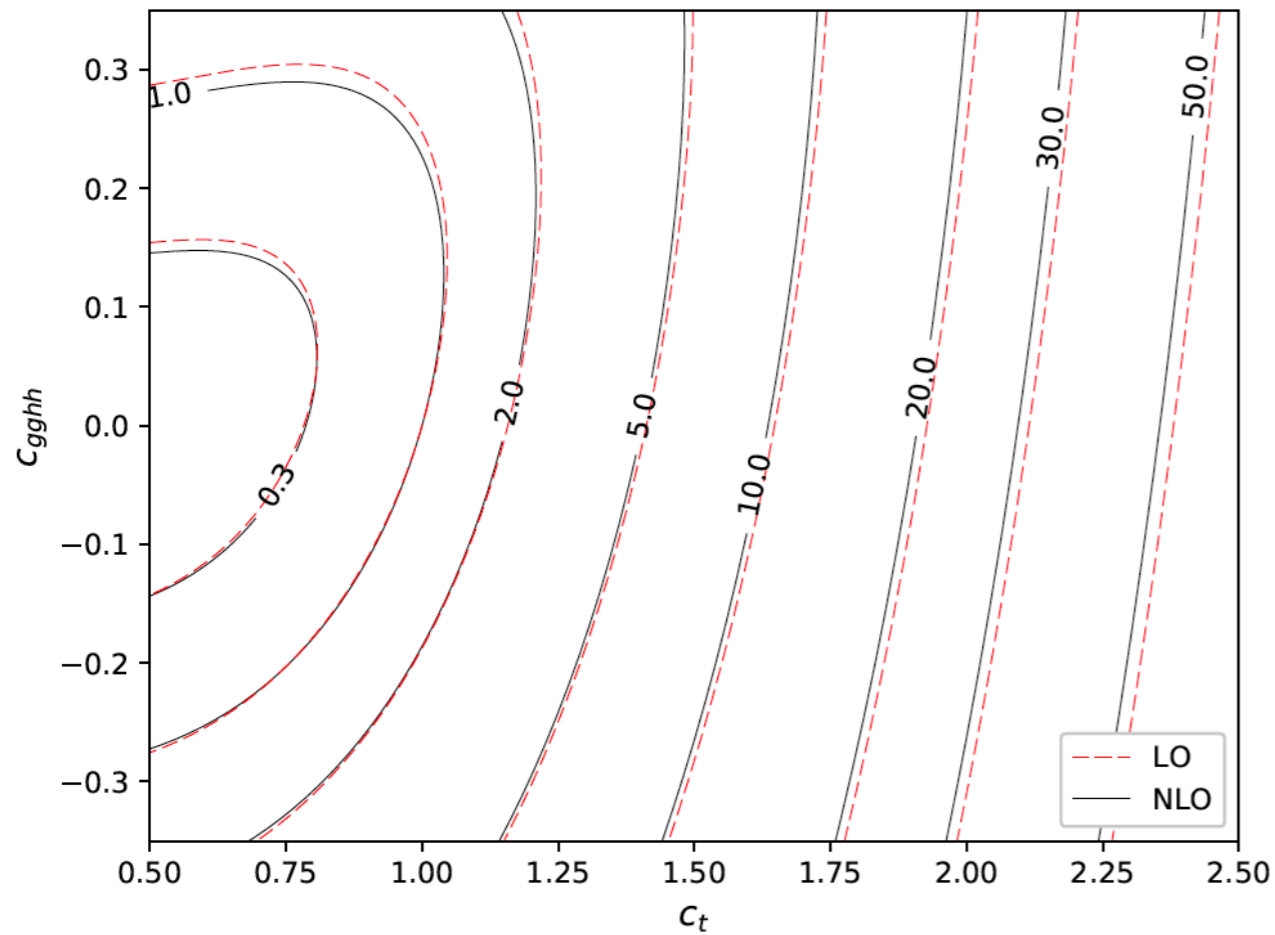
- Small deviations of c_{tt} can lead to big cross section values.
- Deviations of c_{hhh} , more in the negative region than in the positive, lead to enhancement.

NLO Iso-contours



- Changes of c_t to values bigger than 1 can lead to considerable enhancements.
- The total cross section is not very sensitive to the interaction coupling c_{ggh} .

NLO Iso-contours

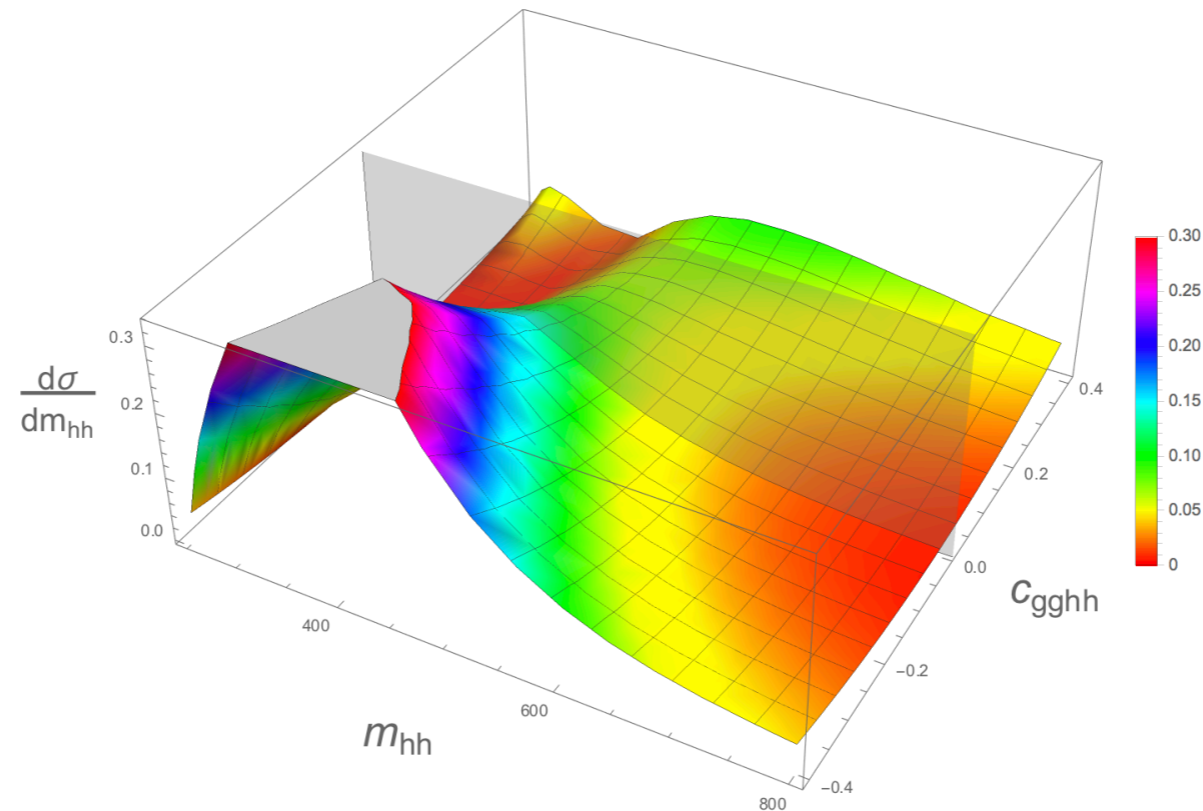
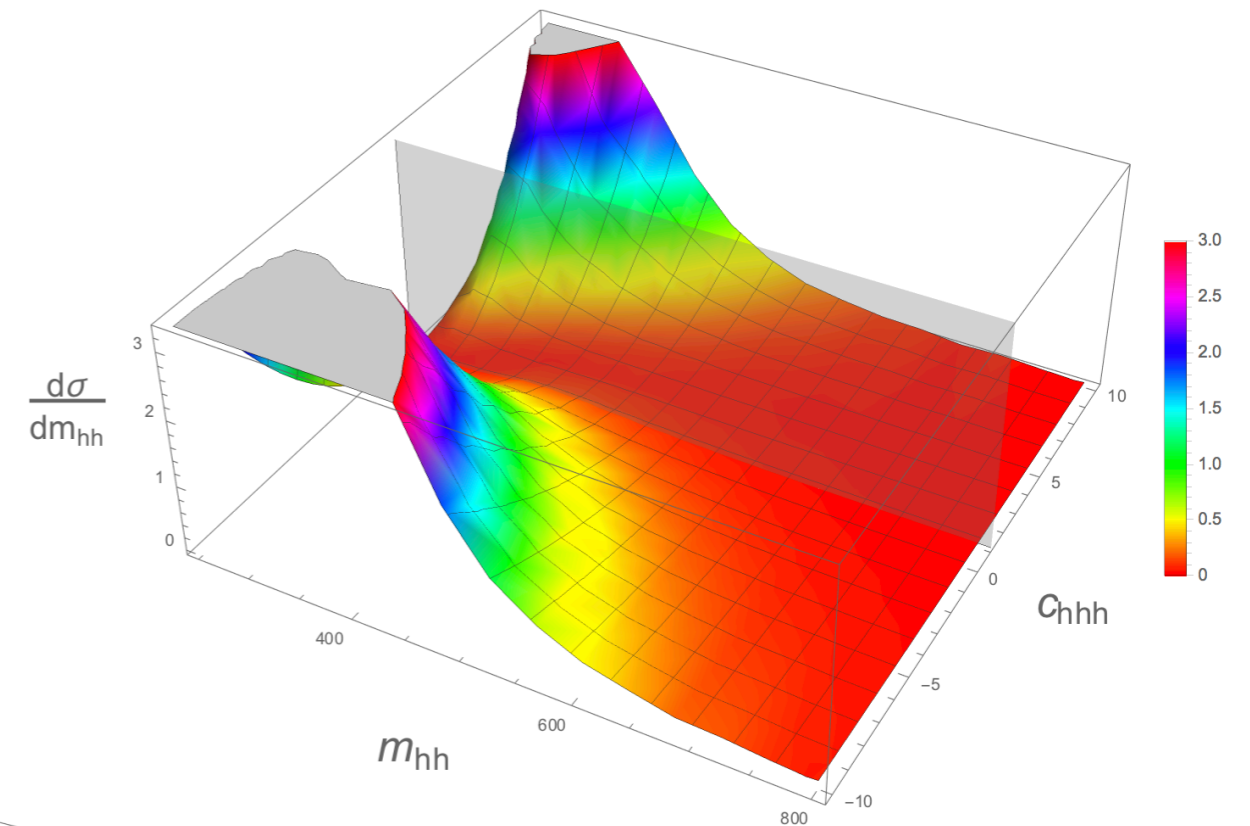
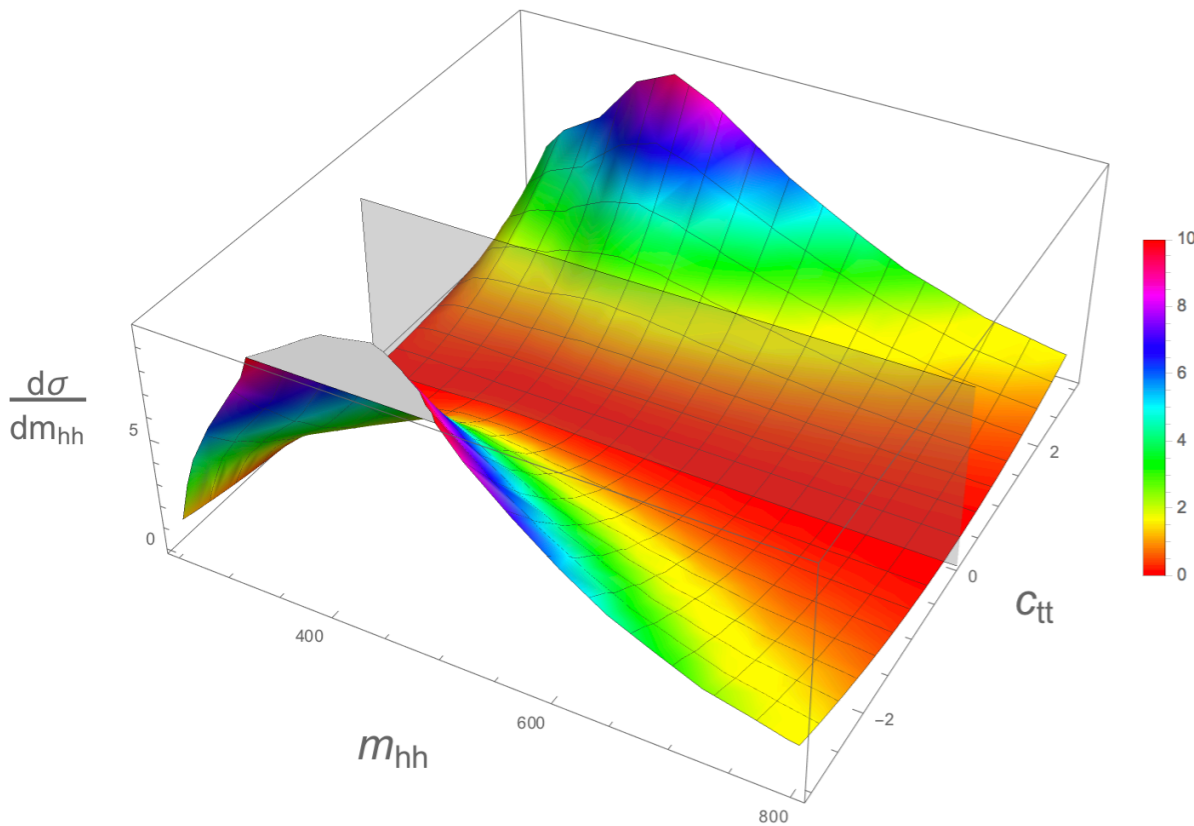


- Variations of the two direct Higgs-gluon couplings do not yield important modifications of the total cross section values.

NLO 3D plots

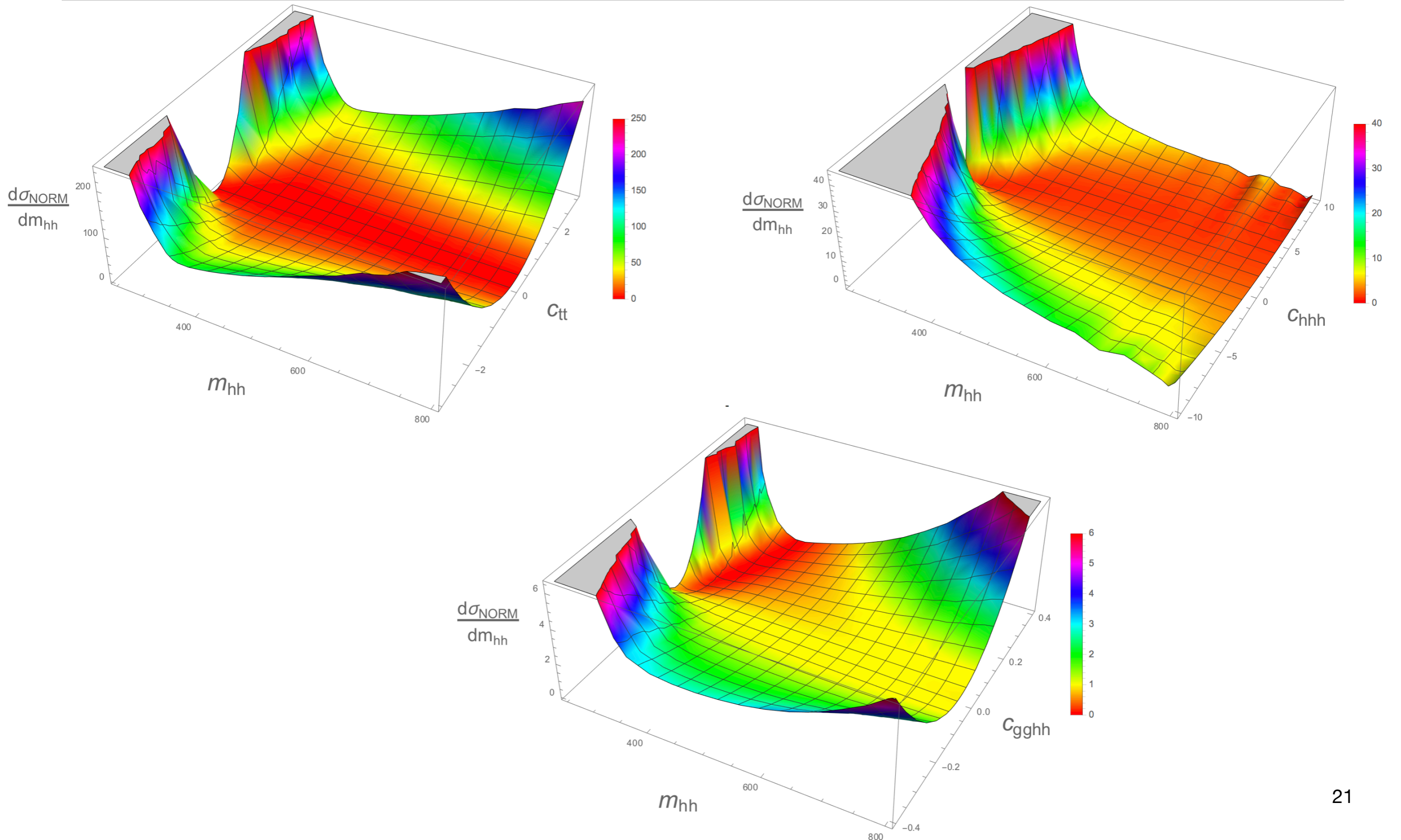
- We performed the fit also at differential level, attached as ancillary files to [1806.05162](#).
- We used the differential fit to produce 3D plots.
- From the 3D plot one can understand the behavior of the differential distribution changing one of the BSM parameters.
- We made a study of the behavior of the differential m_{hh} cross section as a function of the 3 couplings which are difficult to constrain from other processes.
- In each plot we varied just one coupling in a range allowed by experimental constraints, fixing the others to the SM values.

NLO 3D plots



The planes cut on the standard model distributions

NLO 3D plots normalized to the SM



Conclusions

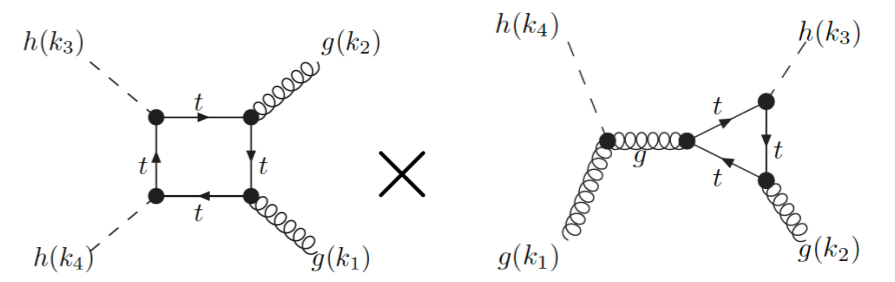
- We computed NLO QCD corrections for Higgs boson pair production in the gluon fusion channel within the EWChL framework. We worked within a five dimensional parameter space.
- We evaluated the full top mass dependent cross sections and differential m_{hh} and p_T distributions for 12 benchmark points up to NLO QCD.
- The analyzes show that in a BSM framework the differential cross section can deviate substantially from the SM prediction. The total cross section can be different from the SM one or almost degenerate; studying the differential cross section allows to break the degeneracy.
- The values of the total cross sections change more rapidly with c_{tt} , c_{hhh} , c_t than with c_{ggh} and c_{gggh} .
- We studied the behavior of the total and differential cross section as a function of the 3 parameters which are difficult to constrain from other processes.
- We gave a parameterization of the total and differential m_{hh} cross section (available as ancillary files) in terms of 23 coefficients which can allow experimentalists to make further analysis.

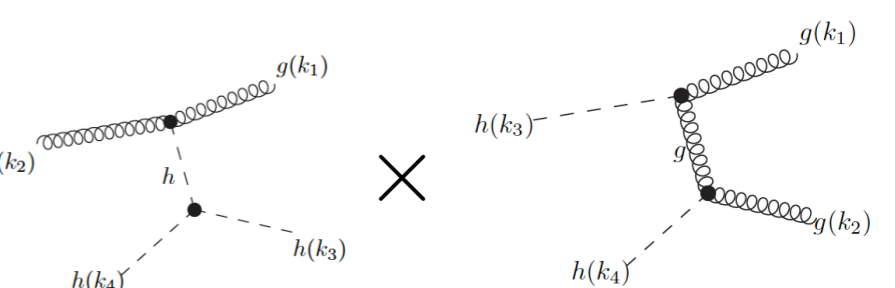


BACKUP SLIDES

Virtual contributions to NLO coefficients

- In order to evaluate the virtual coefficients of the parametrization formula we used a different approach.
- In our setup for the virtual corrections we can isolate the contribution of each diagram to the form factors.
- So we can compute each interference and determine directly all the 23 coefficients.

$$A_{16} \propto$$


$$A_{22} \propto$$


$$A_{23} \propto$$
